EVOLUTION OF THE EARLY SEASON SNOW COVER IN THE COLORADO ROCKIES

Hal Hartman*
Snowmass, Colorado

ABSTRACT: Thirty years of empirical evidence gathered in the Colorado Rockies suggest the frequent development of three distinct layers embedded within the basal layer of the snow cover. Although these layers consist exclusively of depth hoar formed at high growth rates under the influence of strong temperature gradients, on occasion they have appeared independent of initial deposition characteristics. That is, despite the influence of atmospheric conditions on crystal structure during precipitation, a predictable snow cover stratigraphy evolves. In support of empirical evidence, a decade of ram resistance profiles recovered from a high elevation snow study site has been normalized such that a single composite ram resistance profile results. Furthermore, I consider the early season snow cover as a system in thermal and diffusive contact and construct a simple vapor transport model which mimics the aforementioned findings.

Keywords: predictable, normalized, composite ram profile, kinetic metamorphism

1. INTRODUCTION

Excessive snow cover temperature gradients result when episodic storm fronts depart the central Colorado Rockies and leave unseasonably cold arctic air behind. In fact, vertical bulk temperature gradients often exceed $50ºC \cdot m^{-1}$ while vertical near surface temperature gradients commonly surpass $225ºC \cdot m^{-1}$. Also, once the atmosphere becomes cloud free, the snow cover heats the air at rates frequently exceeding 230 $W \cdot m^{-2}$.

Coupling excessive snow cover temperature gradients with a high porosity and shallow snow cover results in rapid conversion of new snow shapes directly to kinetic growth forms. This process is sustained provided unusually dry and cold early season weather patterns characteristic of a high continental climate persist for several weeks.

Empirical evidence gathered by the author over the past 30 years suggests that three distinct layers of depth hoar develop when the aforementioned conditions exist. Furthermore, these layers are found at approximately the same vertical height above the ground from year to year.

Quantitative measurements also support empirical evidence. For example, 10 years of ram penetrometer data recovered from a high elevation snow study site located at the Snowmass Ski Area show that basal layer stratigraphy evolves constant with height. Moreover, ram resistance profiles resemble empirical knowledge of the author and the Snowmass Ski Area avalanche risk management crew.

Calculation of water vapor density given snow cover temperatures recovered from the previously mentioned snow study site indicate that the vertical concentration of water vapor regularly varies by a factor of 12. Consequently, application of Fick's Law demonstrates that vapor diffusion is preferentially removing and depositing ice at specific locations within the snow cover; indeed, the densification rate curve generated by this simple one dimensional vapor transport model mimics empirical and quantitative findings.

Finally, the author and the Snowmass Ski Area avalanche risk management crew have long believed that collapse of the basal layer of depth hoar is exclusively initiated from overlying soft and hard slabs. However, it now appears possible that stress applied by low density snowfall may exceed the shear strength of these layers and that the coincident rate of deformation is sufficient to initiate shear fracture within the basal layer of depth hoar.

2. STUDY SITE

Located in the central Colorado Rockies, the Snowmass Ski Area includes avalanche terrain consisting of two small glacial cirques and an extensive source area for blowing and drifting snow. Moreover, a relatively cold and dry continental climate (Hartman, 1994) dominates early winter weather conditions.

Within the boundary of the Snowmass Ski Area, the TLS study site and the BLD weather station in combination with an archive of daily weather reports,

* *Corresponding author address:* Hal Hartman, P.O. Box 474, Snowmass, CO 81654.

field observations and avalanche occurrences of some 37 years provide the foundation for avalanche risk management.

At an elevation of 3550 m the TLS snow study site is located on a north facing aspect. Here an array of sensors measure: Ground, snow cover, snow surface, and air temperatures; relative humidity; net radiation; water equivalent from precipitation; 24 hour snowfall height; and total snow cover height. Data are acquired by a CR10 datalogger, processed, stored and downloaded on demand via phone link. Also, as of December 1991 this site supports most formal snow profile observations including systematic application of a standard ram penetrometer.

The BLD weather site is located at ridge crest. At an elevation of 3870 m air temperature, wind velocity, relative humidity, shortwave radiation, and barometric pressure measurements are acquired by a CR10 datalogger. This data is then processed, stored and downloaded via radio link.

3. METHODS

3.1. *Empirical methods*

Records consisting of 512 hasty and full data snow pits recorded by the author and 480 hasty and full data snow pits recorded by members of the Snowmass Ski Area avalanche risk management crew serve as empirical evidence. They range in detail from sketches of hand hardness profiles to observations typical of formal snow profiles (McClung and Schaerer, 1994).

For example, snow cover observations were conducted to determine if layers of low density snow were being converted to faceted shapes. The location of these layers relative to the ground, crusts, soft and hard slabs in addition to their tendency to collapse or shear was recorded.

Faceted particles were examined with a magnifying lens, typed, and sized according to the largest observed particle. Finally, if time permitted snow density measurements, temperature and hand hardness profiles were obtained.

3.2. *Quantitative measurements*

Seldom does the early season snow cover possess enough strength to yield a standard ram penetrometer resistance profile. Consequently, a lightweight ram penetrometer (Armstrong, 1980) with approximately 1/10 the mass of a standard ram penetrometer was constructed.

Following fabrication of the lightweight ram penetrometer, cross sections of the hole created by the lightweight ram revealed that depth hoar crystals were accumulating on the upper surface of the conic section. Consequently, top surface geometry was reconfigured resulting in an 8.2 percent reduction in surface area. Having altered internationally accepted dimensions, a correction factor was determined (Brun and Rey, 1987).

Within a 2 by 6 meter grid, 11 consecutive lightweight ram penetrometer resistance profiles were obtained from the upper 0.5 meters of the snow cover. Each lightweight ram penetrometer test was conducted by the same observer.

Next, from the net force required to drive the lightweight ram 0.5 meters into the snow cover in each of the 11 samples, the coefficient of variation (Jamieson, 1995) was found to be 7.2 percent. Therefore, the lightweight ram penetrometer was deemed capable of consistently measuring small incremental changes in the mechanical state of the snow cover (Landry, 2002).

After final adjustments and familiarization with the lightweight ram penetrometer, the Snowmass Ski Area avalanche risk management crew commenced a concentrated series of observations. Over the duration of a winter season, one lightweight ram penetrometer test and a concurrent formal snow profile were obtained every 3 days at the TLS study site. Moreover, during the next winter season, 2001 / 2002, procedures followed those just mentioned except data were obtained every 10 to 14 days.

Composite ram penetrometer resistance profiles were generated from 26 standard and lightweight ram penetrometer tests. These tests were conducted over a 10 year period when snow cover depth ranged between 0.73 and 1.06 meters. The vertical coordinate was normalized by dividing ram penetrometer penetration by total snow cover height and subtracting the quotient from 1. The horizontal coordinate was normalized by dividing the ram penetrometer value by the mean ram resistance value. Finally, data were sorted into bins given specific increments: 0.1 for the standard ram penetrometer and 0.06 for the lightweight ram penetrometer. Values were then statistically analyzed, averaged and plotted.

3.3. *Mathematical Modeling*

Ground temperature at the TLS study site remains at the meting point of ice throughout winter. Coincident temperature at the snow / air interface, although variable due to dependence on atmospheric conditions, frequently measures 25 degrees less than the temperature of the underlying ground; Figure 1 depicts this condition.

Calculation of water vapor density within a

porous snow cover is possible given temperature, water vapor pressure over ice and application of the ideal gas equation. Thus, referring to the snow cover temperature profile found in Figure 1, vapor density is 4.9 g·m^{-3} near the ground and 0.41 g·m^{-3} near the snow surface. This suggests that the concentration of water vapor is 12 times greater near the ground than it is near the surface of the snow cover.

Fick's Law states that a diffusing substance, such as water vapor, will move from a region of high concentration to a region of low concentration. However, diffusion of water vapor from a basal layer to a near surface layer of the snow cover requires a minimum bulk temperature gradient of ten degrees Celsius per meter of snow cover height (LaChapelle, 1969).

Once water vapor is mobilized, the solid to vapor—vapor to solid process of sublimation relocates ice from regions near the ground to regions near the snow cover surface. The end result is a snow cover comprised of kinetic crystal growth forms (Akitaya, 1974) in various stages of development.

Finally, the aforementioned principles provide the underpinning for derivation of a single dimension vapor transport model.

3.4. *Vapor transport model assumptions*

1. Bulk temperature gradient dominates macroscopic vapor diffusion. Whereas water vapor diffusion patterns given microscale ice particle geometry are ignored.
2. Given Fick's law (Colbeck, 1982)

$$J = D_{eff} \frac{\partial \rho}{\partial z} \tag{1}$$

the vapor diffusion constant, D_{eff}, as described by Sokratov (2002) is superior to Colbeck's (1993) enhancement factor L.

3. The ideal gas equation coupled with data found in the *Handbook of Chemistry and Physics* describing water vapor pressure over ice provides an accurate representation of water vapor density within the snow cover.
4. Empirical evidence and composite ram resistance profiles determine the sense of equation (1).

3.5. *Calculation of water vapor density*

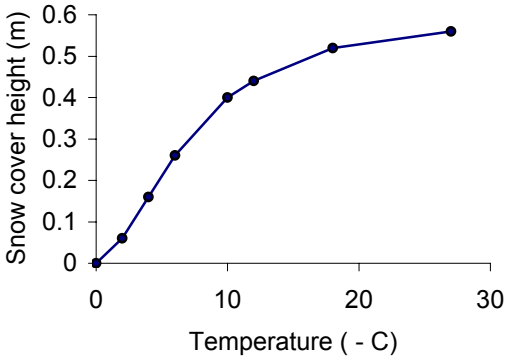

Figure 1: Snow cover temperature gradient profile recorded on December 14, 2000 at the Snowmass Ski Area.

The ideal gas equation, as applied to individual gaseous components of air, may be written

$$e\alpha_V = R_V T \tag{2}$$

where e and α_v are the vapor pressure over ice and specific volume of water vapor (Wallace and Hobbs, 1977). The value of R_v is given by

$$R_V = \frac{R_U}{M_W} \tag{3}$$

where R_U is the gas constant for one kilogram of water vapor and M_w is the molecular weight of water. Thus, equation (2) permits the calculation of the specific volume of water vapor pressure over ice. Therefore, the density of water vapor over ice is given by

$$\rho_V = \frac{1}{\alpha_V} \tag{4}$$

Finally, fitting an exponential curve of the form

$$\rho_{(V)} = Ae^{BT} \tag{5}$$

to the values generated by equation (4) permits calculation of water vapor density given snow cover temperature.

3.6. *Temperature as a function of snow cover height*

Next, fitting the temperature profile found in Figure 1 with a fourth order polynomial

$$T_{(Z)} = \left(Az^4 + Bz^3 + Cz^2 + Dz + E\right) \cdot K \qquad (6)$$

yields temperature as a function of snow height.

3.7. *Diffusion coefficient*

After Sokratov (2002) the diffusion coefficient D_{eff} found in equation (1) is

$$D_{eff} = D_a \frac{\psi}{\tau} \qquad (7)$$

where ψ is areal porosity of snow and is given by

$$\psi = 1 - \frac{\rho_{meas}}{\rho_{ice}} \qquad (8)$$

ρ_{meas} is the average bulk density of the snow cover concurrent to Figure 1 and ρ_{ice} is the density of ice. Tortuosity, τ, is 1.7 for snow at 300 kgm^{-3} which accounts for the blockage of vapor by snow particles embedded in the snow cover. Finally, D_a is the diffusion coefficient and is given by

$$D_a = \left[D_{air} \left(\frac{P_o}{P} \right) \left(\frac{T}{T_o} \right) \right]^{1.81} \qquad (9)$$

Here, D_{air} is the diffusion coefficient of water vapor in air, P_o is atmospheric pressure at sea level, P is standard pressure at 3500 m above sea level, T_o is the temperature of melting ice at one atmosphere, T is equation (6) and the power 1.81 is a correction factor based on in situ measurements (Sokratov, 2002).

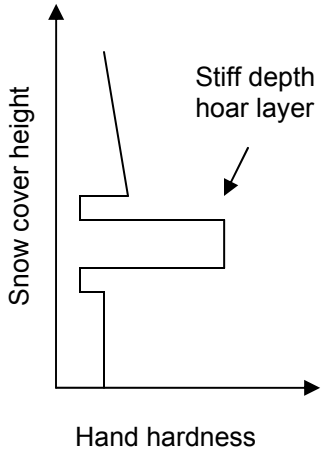

Figure 2: Idealized sketch representing empirical knowledge. Of primary importance is the alternating soft—hard—soft region centered at the stiff depth hoar layer.

3.8. *Vapor diffusion model output*

Equation (1) may be used to describe water vapor diffusion in snow. Therefore, taking the partial derivative with respect to height, *z*, gives

$$\frac{\partial J_V}{\partial_Z} = D_{eff} \frac{\partial^2 \rho_V}{\partial z^2} \qquad (10)$$

which is the rate of water vapor diffusion within the snow cover expressed in kg·m^{-3}·s^{-1}. Sturm and Benson (1997) derive similar results.

4. RESULTS

4.1. *Empirical results*

As early winter unfolds new snow shapes found in a porous shallow snow cover which is dominated by excessive snow cover temperature gradients convert directly to faceted particles.

Within weeks two extremely weak layers of depth hoar develop below and above a stiff layer of depth hoar. This stiff layer of depth hoar is easily found by application of a hand hardness test and is the dominant region of hardness identified in Figure 2; rarely does the hand test yield values greater than four fingers.

As mid winter approaches, if snow cover height

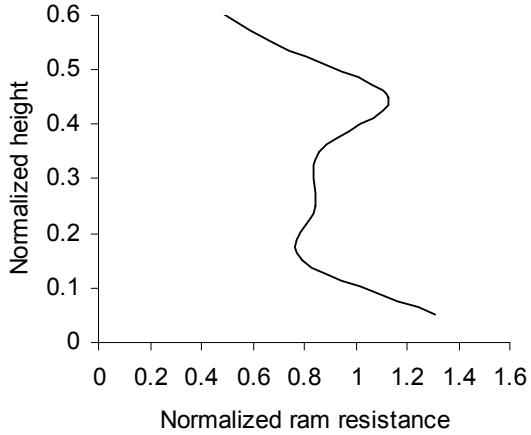

Figure 3: Composite standard weight ram resistance profile.

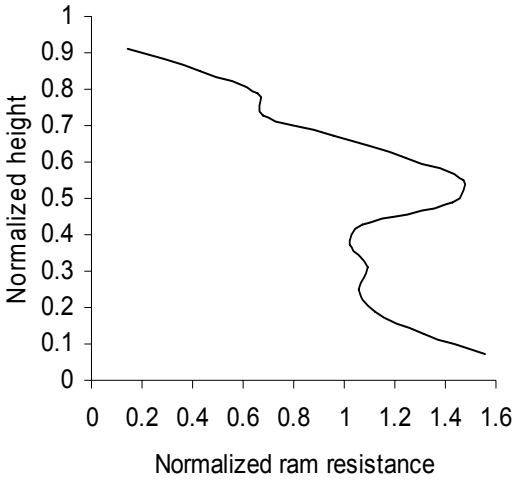

Figure 4: Composite lightweight ram penetrometer resistance profile.

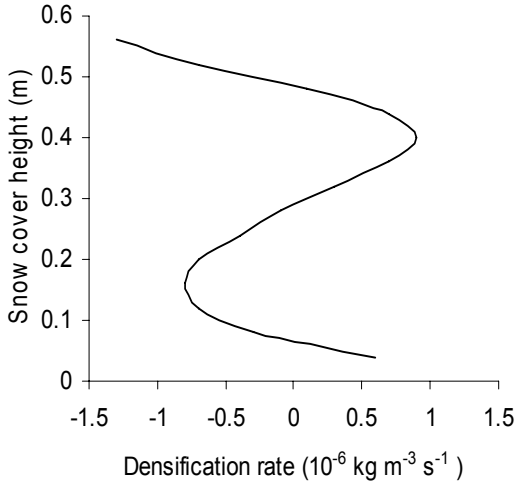

Figure 5: Calculated vapor diffusion at the TLS study site on December 14, 2001.

reaches 1.2 m, then excessive snow cover temperature gradients relax. Subsequently, basal layer temperatures approach 0º C and an overall net loss of strength occurs in the first meter of snow cover height.

4.2. *Quantitative results*

Quantitative findings are presented graphically in Figures 3 and 4. The curve found in Figure 3 is a composite of 14 standard ram penetrometer tests collected at the TLS study site over an 8 year period when snow cover height ranged from 0.73 to 1.06 meters.

Likewise, the composite lightweight ram profile found in Figure 4 was generated from 12 lightweight ram penetrometer tests collected over a 2 year period at the TLS study site when snow cover height ranged from 0.87 to 1.05 meters.

4.3. *Vapor transport model results*

Calculated vapor diffusion on December 14, 2002 is presented graphically in Figure 5. Here, given model assumptions, vapor diffusion is preferentially removing mass at 0.2 meters and depositing mass at 0.4 meters.

5. DISCUSSION

Empirical, quantitative and theoretical evidence have been generalized. For example, the hand hardness sketch in found in Figure 2 represents the author's best attempt at describing early season snow stratigraphy based on 30 years of field experience. The region of idealized alternating layers of soft—hard—soft depth hoar is the important feature in this sketch.

Equally important are ram penetrometer data spanning one decade; here, it is the shape of the composite ram profiles found in Figures 3 and 4 which are important. They indicate that under previously mentioned conditions, a stiff layer of snow can typically be found at a distance above the ground which is proportional to snow cover height (Jamieson, 2004).

Furthermore, the shape of the densification rate curve found in Figure 5 mimics empirical and quantitative results. Here, it is believed that an increase in mass due to preferential deposition of ice at 0.4 m above the ground corresponds to the hard layer of depth hoar pointed out in Figure 2. Likewise, the densification rate curve corresponds to spikes in normalized ram resistance at approximately 0.5 on the y-axis found in Figures 3 and 4.

Figure 6 serves as example of field observations collected by members of the Snowmass Ski Area Avalanche risk management crew. Pit # 10 is a fracture line profile. Here alternating layers consisting of soft—hard—soft depth hoar begin 25 cm above the ground. This particular snow pit was selected for purposes of demonstrating that not always will field observations clearly represent the idealized sketch found in Figure 2.

6. CONCLUSION

LaChapelle (1980) mentions that the fundamental avalanche forecasting process includes "a high level of skill developed through empirical

experience." He also claims that this process as actually practiced relies on repetitive reasoning in which general principles are derived from facts or instances. Thus in terms of conventional avalanche forecasting, the empirical data although difficult if not impossible to quantify are considered significant.

Normalizing vertical and horizontal ram penetrometer coordinates show that from year to year the position of snow layers above the ground is often times proportional to height (Jamieson, 2004). However, composite ram resistance profiles demonstrate that over a 10 year period a general snow cover stratigraphy evolves. Although these layers consist exclusively of depth hoar formed at high growth rates under the influence of strong temperature gradients, on occasion they have appeared independent of initial deposition characteristics. Consequently, quantitative evidence is considered equal in significance when compared to empirical findings.

Error analysis points out two weaknesses associated with the simple one dimensional vapor transport model: First, application of the ideal gas law regarding calculation or vapor density over ice and second, Sokratov's tortuosity value given bulk snow cover density of 300 $kg \cdot m^{-3}$. Regarding the former, once the ideal gas equation was written for an individual gaseous component, water vapor in this instance, density values approximated those calculated by Sturm and Benson (1997). About the latter, critical early winter snow cover bulk density measurements range between 180 $kg \cdot m^{-3}$ and 220 $kg \cdot m^{-3}$. Consequently, if tortuosity were a linear relationship, then by ratio a value of 1.13 would be a better approximation given an average snow cover bulk density of 200 $kg \cdot m^{-3}$. Nevertheless, vapor model output given smaller values of tortuosity did not change the form of the densification rate curve found in Figure 5. Theoretical evidence, although valuable, as compared to empirical and quantitative findings is considered least in terms of significance.

Finally, empirical, quantitative and theoretical evidence indicate that the first meter of the snow cover has a high probability of tending toward a particular stratigraphy. It is here that extensive field observations indicate shear like behavior. Considering mechanical behavior it appears likely that stress applied by low density snowfall may exceed the shear strength of these layers. Furthermore, coincident rates of deformation may be sufficient to initiate shear fracture thus incite avalanche release from within the basal layer of depth hoar.

7. ACKNOWLEDGEMENTS

I gratefully acknowledge the assistance of the Snowmass Ski Area avalanche risk management crew. They are a talented group of people who begin and end each day with a "can—do" attitude. Finally, thanks to Chris Landry and Bruce Jamieson for reviewing portions of this manuscript.

8. REFERENCES

Akitaya, E. 1974. Studies on depth hoar. Cont. Inst. Low Temp. Sci. Ser. A26. p 48.

Armstrong, R.L. 1980. An analysis of compressive strain in adjacent temperature-gradient and equi-temperature layers in a natural snow cover. Journal of Glaciology. Vol. 26, No. 94, p. 283-289.

Brun, E. and L. Rey. 1987. Field study on snow mechanical properties with special regard to liquid water content. International Association of Hydrological Sciences. Publication No. 162, p. 183-193.

Colbeck, S.C. 1993. The vapor diffusion coefficient for snow. Water Resources Research. Vol. 29, No. 1, p. 109-115.

Hartman, H. 1994. Forecasting high continental avalanches: A field workers perspective. Proceedings of the International Symposium on Snow and Related Manifestations. Manila, India. p. 425-429.

Jamieson, B. 1995. Avalanche Prediction for Persistent Snow Slabs. PhD Thesis. Univ. of Calgary, Alberta, Canada, 258 pp.

Jamieson, B. 2004. Personal communication.

LaChapelle, E.R. 1969. Field Guide to Snow Crystals. University of Washington Press. 101 pp.

LaChapelle, E.R. 1980. The fundamental processes in conventional avalanche forecasting. Journal of Glaciology. Vol. 26, No. 26, p. 283-289.

Landry, C. 2002. Personal communication.

McClung, D.M. and P. Schaerer. 1993. The Avalanche Handbook. Seattle, WA, The Mountaineers. 271 pp.

Sokratov, A. 2002. Personal communication. Swiss Federal Institute for Snow and Avalanche Research, Davos, Switzerland.

Sturm, M. and C. Benson. 1997. Vapor transport, grain growth and depth-hoar development in the

subarctic snow. Journal of Glaciology. Vol. 43, No. 143. p. 42-59.

Wallace, J.M. and P. V. Hobbs. 1977. Atmospheric Science. University of Washington, Academic Press. p 50.

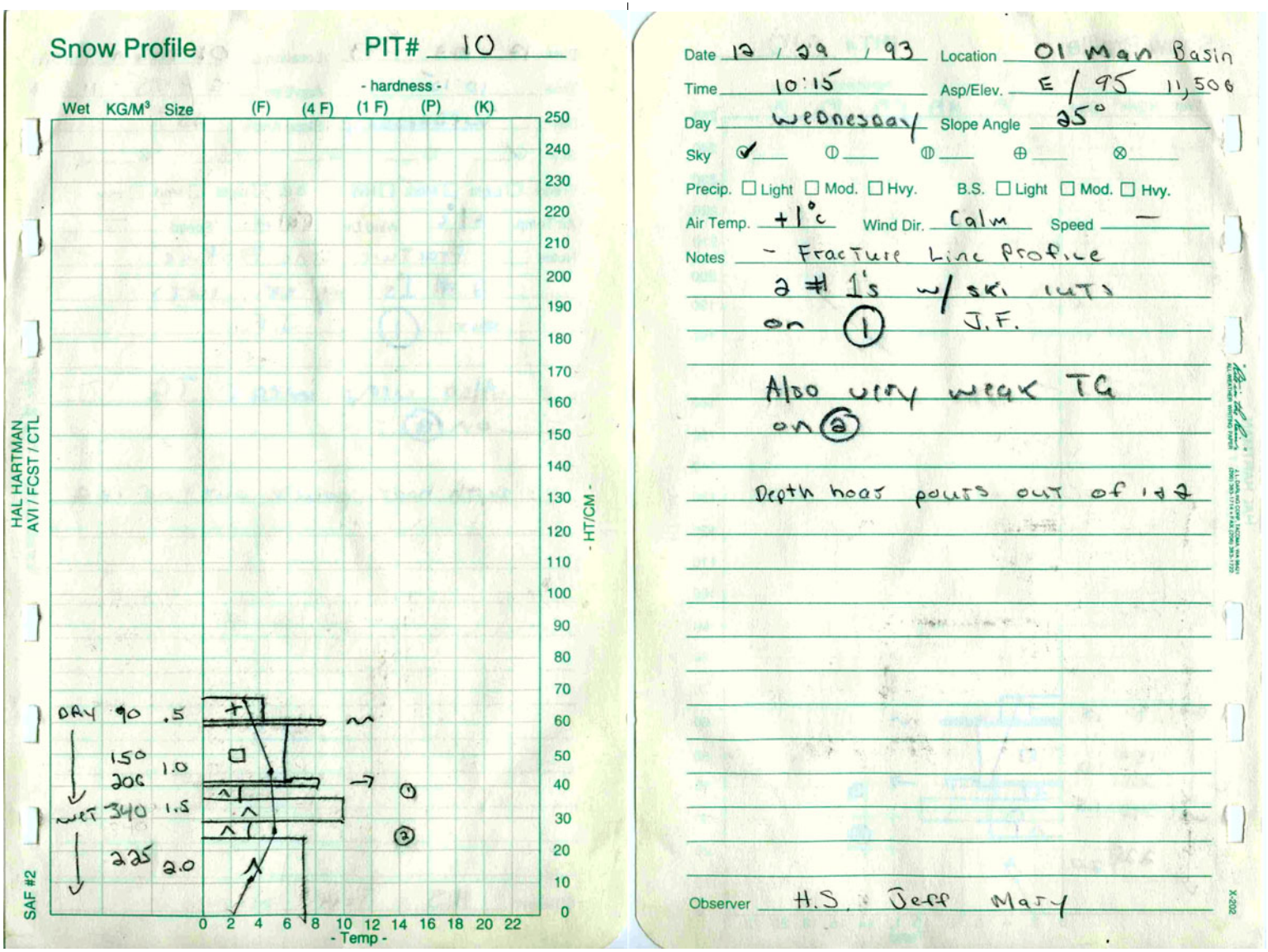

Figure 6: Pit # 10, fracture line profile collected by members of the Snowmass Ski Area risk management crew, demonstrates the presence of alternating layers of soft-hard-soft depth hoar centered at 35 cm above the ground.